

Relationships between Polymorphic Crystals and Multiple Melting Peaks in Crystalline Syndiotactic Polystyrene

Ya Sen Sun and E. M. Woo*

Department of Chemical Engineering, National Cheng Kung University, Tainan, 701-01, Taiwan

Received April 6, 1999

ABSTRACT: Multiple crystal forms and complex melting behavior of syndiotactic polystyrene (sPS) were thoroughly examined using wide-angle X-ray diffraction (WAXD) and differential scanning calorimetry (DSC). This study has provided clear evidence for interpretation of relationships between the multiple melting peaks and polymorphic crystals in sPS under isothermal melt-crystallization, dynamic cooling, or other thermal histories. For the first time, assignment of different crystal types to the numerous melting peaks in sPS was accomplished. Effects on the mechanism of chain packing were examined for correlating the relationships between the polymorphism and multiple melting peaks. The α -crystal packing can be favored and becomes an alternative route in sPS crystallization under three conditions: (1) slow cooling from molten state, (2) melt crystallization at low temperatures, or (3) cold crystallization from quenched amorphous glass. By comparison, melt-crystallization at most accessible temperatures produces solidified sPS containing both α -type and β -type crystals of various fractions, but a higher temperature tends to favor greater fractions of β -type crystal. The β -type crystal becomes the only discernible species if sPS is melt-crystallized at temperatures equal to or higher than 260 °C, which suggests that in conditions approaching equilibrium the β -crystal lamella is the favored packing in sPS.

Introduction

Crystal forms and effects on polymorphic behavior of syndiotactic polystyrene (sPS) are known to be complex. Although there have been numerous studies on various sPS topics, multiple melting peaks in possible correlation with particular crystal forms in sPS have yet to be understood. Earlier studies in this laboratory¹ and other recent reports in the literature have demonstrated that there are three identified sharp melting peaks (peaks 1, 2, and 3) for the melt-crystallized sPS samples but only one broad and irregularly shaped peak for the cold-crystallized sPS (when scanned at 10 °C/min). sPS is a fast-crystallizing polymer, and processing histories can sensitively influence its microstructures and properties. Many studies have been devoted to understand the relationships between processing and structure in sPS. Compression-molding under high a pressure was proposed to lead to mainly the β -crystal in sPS.² Additionally, formation of the β -form is proposed to be favored over the α -form in sPS by solvent casting at high temperatures.³ Thermal histories and/or temperature of crystallization can have profound effects. Guerra and De Rosa et al.^{4–6} also found that crystallization of sPS from melt produces different fractions of α - and β -forms depending on cooling rate. In addition, recent studies pointed out that melt-crystallization at high temperatures preferentially favors the formation of the β -form.^{1,7,8} Upon melt-crystallization at several isothermal temperatures between 230 and 250 °C, the relative fraction of the two types of crystals can change. The β -form crystal may become a more preferable way of packing over the α -crystal for the sPS crystallized/annealed at higher temperatures closer to T_m .⁸ Through-thickness variation of structure and morphology in injection-molded sPS is possible as differences in thermal histo-

ries lead to variation of relative proportions of these two crystal types.⁹ Previous studies already demonstrated that X-ray characterization on the cold-crystallized sPS ($T_{cc} = 200$ –260 °C) contained only the α -crystal (or majority).¹ Cold-crystallization (from quenched amorphous glass) at temperatures higher than 200 °C (200–250 °C) has been found to produce only the α -crystal. By a significant contrast, melt-crystallization (from the molten state of sPS) produced either a combination of α -type and β -type crystals at lower temperatures (240 °C or lower) or a majority of β -type if at temperatures higher than 260 °C. Melt-crystallization of sPS at different temperatures can lead to crystalline phases that exhibit dramatically different melting behavior. In addition to possible crystal–crystal transformation, at higher crystallization temperatures, the mechanism of α -form packing is less favored than the β -form packing for molten sPS being crystallized. The fact suggests that the dominating crystal forms are different, and their relative fraction depends on thermal/processing histories. Note that both α - and β -crystals are of a planar zigzag chain conformation, but the β -crystal is packed into an orthorhombic unit cell with $a = 0.88$ nm, $b = 2.88$ nm, and c (chain axis) = 0.51 nm,^{3,4} while the α -crystal is of a hexagonal unit cell.

Interpretation of multiple melting peaks in semicrystalline polymers has been difficult and lacking a clear conclusion in the past two decades. Wunderlich¹⁰ has proposed a mechanism of double melting by theorizing on melting of the minor crystal and recrystallization and remelting during scanning, while much earlier Roberts¹¹ has explained this behavior in terms of the melting of crystals of two different sizes. Poly(ether ether ketone) (PEEK), as an example, is one of the most studied subjects. A reorganization model^{12,13} suggests that lamellae can be reorganized quickly enough to thicker ones during the time frame of scanning. By contrast, a dual-morphology model^{14–16} suggests that secondary lamellae may melt at lower temperatures and the

* To whom correspondence is to be addressed. Fax +886 6 234-4496; e-mail emwoo@mail.ncku.edu.tw; phone +886 6 275-7575, ext. 62670.

primary lamellae melt at higher temperatures. In addition, experimental evidence (polarized optical microscopy) for two coexisting different lamellar morphologies has also been proposed.^{17,18} Although the reorganization mechanism cannot be completely ruled out, its applicability in accounting for the dual or multiple melting peaks may depend on the time frame of scanning.¹⁹ Upon extended annealing or within a longer time frame of scanning (e.g., extremely slow scan rates), reorganization may be more likely. A later modification of reorganization and dual morphologies has proposed that preexisting multiple lamellar thicknesses and their changes upon scanning/annealing can be found in poly(ether ether ketone) (PEEK).²⁰

Since the discovery of successful synthesis of highly stereoregular sPS in 1986,²¹ it has been widely studied on many topics including its complex morphology.^{1-9,22-25} Various analyses by many researchers have led to in-depth understanding of crystal types present in sPS subjected to different thermal histories or states; however, relationships between crystal morphology and multiple melting behavior are yet to be clarified. In continuing our previous published work,^{1,8} the objective of this study was to examine how individual crystal forms in sPS may be related to the multiple melting peaks in melt-crystallized sPS. Furthermore, assignment of these melting peaks to individual crystals was attempted. Miscibility in sPS blends with atactic polystyrene (aPS) has been demonstrated in a recent paper.²⁶ More in-depth understanding was gained by examining relationships between polymorphism and melting behavior of neat sPS in direct comparison with miscible sPS blend samples.

Experimental Section

Materials and Procedures. Semicrystalline syndiotactic polystyrene (sPS) was obtained as a courtesy sample material from Idemitsu Petrochemical Co., Ltd. (Japan), with $M_w = 241\,000$ g/mol and $PI (M_w/M_n) = 2.3$ and T_g (onset, at 20 °C/min) of 95 °C. The supplier-furnished data of percent syndiotacticity of the sPS indicates very high tacticity (greater than 95%). The crystallinity (by X-ray) of sPS (as-received) was not performed as the crystallinity of the sample is highly dependent on the thermal histories. To eliminate additional thermal effects of changing T_g , the ideal polymer component for forming mixtures with sPS should possess approximately the same T_g . Atactic polystyrene (aPS) was chosen (Chi-Mei, Inc., Taiwan), $M_w = 237\,000$ g/mol (GPC), $PI = 3.1$, and T_g (onset) of 87.5 °C. Note that the MW's of aPS and sPS used in this study are comparable. Hot-melt mixing was used for preparing blend samples of sPS with aPS. The constituent polymers (1:1) were ground into fine powder, dried, and premixed and melt-blended at 320 °C.

Samples (neat sPS and aPS/sPS blends) of various thermal histories were prepared. Isothermal melt crystallization/annealing of various time duration were performed on samples by placing the samples directly in a differential scanning calorimeter to ensure temperature accuracy. After going through designated thermal treatments, they were ready for either DSC experiment or X-ray characterization. In addition, amorphous sPS (free of initial/residual crystallinity) was used as a starting material for subsequent cold-crystallization at designated temperatures. Because of fast crystallization during cooling transient, crystal-free amorphous sPS material was obtained by the direct quenching to liquid N₂ instead of quenching in DSC cells. Film samples of amorphous sPS was prepared by heating/melting the as-received sPS pellets (originally semicrystalline) to 310 °C, compression-molded into a thin film (between two aluminum-plate molds), then quenched quickly into liquid nitrogen or ice water.

Apparatus. Differential scanning calorimetry (DSC-7, Perkin-Elmer) equipped with a mechanical intracooler was used for determining the melting transition temperatures and enthalpy of melting peaks. The temperature and heat of transition of the instrument were calibrated with indium and zinc standards at 10 °C/min. Heating rates of 2.5, 5, 10, 20, 30, and 40 °C/min were used for different scanning schemes. For melt-crystallization treatments, samples were heated to above melt and quickly cooled (−320 °C/min) in the DSC cell to desired isothermal temperatures (230–260 °C). During thermal annealing or scanning, a continuous nitrogen flow in the DSC sample cell was maintained to ensure minimal sample degradation. The wide-angle X-ray instrument (WAXD) was Rigaku D/Max II-B with copper K α radiation and a wavelength of 1.542 Å. For direct comparison, specimens of X-ray characterization were prepared using the similar thermal treatments as described for the thermal analysis samples.

Results and Discussion

Complex Melting Peaks in sPS. When melt-crystallized sPS samples (at 240–250 °C) were scanned in DSC at a typically regular heating rate of 10 °C/min, at least three distinct melting peaks, labeled peaks 1, 2, and 3, were observed. The assignment of melting peaks (peaks 1, 2, and 3) to possible crystal forms is attempted by many researchers; however, there has been no agreement. There may be less argument on proposals that peak 1 is attributed to the β -crystal, while peak 2 may be associated with melting of the α -type crystal.^{8,27} Direct evidence, however, is still lacking. Furthermore, the origin of peak 3 melting endotherm has not been clear. To make matters more complicated, in this report it will be shown that actually there exist four (not just three) melting peaks in melt-crystallized sPS samples when the DSC resolution is sufficiently good. Thus, the assignment of peak 3 and peak 4 to the crystal types has yet to be explained. DSC characterization showed that a shoulder peak adjacent to peak 3 was present. To enhance the resolution, a slower scanning rate was used in DSC characterization of these isothermally crystallized sPS. When the sample was scanned at slower rates (e.g., 2.5 or 5 °C/min), this shoulder endotherm appeared as a totally separate melting peak (labeled "peak 4"), whose peak temperature is located at greater than 270 °C. Upon melt-crystallized at an even higher temperature (e.g., 260 °C) for 120 min, the samples exhibited no trace of peak 2, leaving only a greatly enhanced peak 1 ($T_m = 272$ °C). In addition, isothermal crystallization at increasingly high temperatures (250–254 °C) led to gradually diminished intensity of peak 3, which eventually disappears if sPS is melt crystallized at high enough temperatures.

To understand which of these melting peaks might be associated with different crystal forms, one must first determine the sequence of growth of crystals. Figure 1a–f shows the DSC traces (all scanned at 5 °C/min) revealing four melting peaks in the sPS samples melt-crystallized at isothermal 240 °C for various times from 0.5 to 120 min. These melting peaks are peaks 1, 2, 3, and 4, located at 260, 264, 270, and 273 °C, respectively. For abbreviation, these melting peaks (from low to high temperature) are alternatively labeled as P1, P2, P3, and P4, respectively. Note that the intensities of these melting peaks vary with the time of holding at melt crystallization. In addition, the sequence of appearance of these peaks may provide some hint. At early times (less than 1 min) of crystallization (at 240 °C), the sPS displays only P1 and P3. The intensity of P1 and P3 is

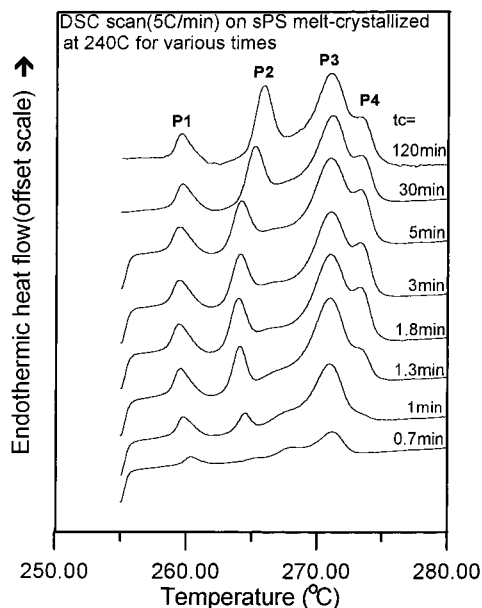


Figure 1. DSC traces (scanned at 5 °C/min) of neat sPS samples melt-crystallized isothermally at 240 °C for various times ranging from 0.5 to 120 min.

more or less fully developed in sPS melt-crystallized for 1.8 min. After the early appearance of P1 and P3, P2 and P4 start to emerge. Only for the sPS samples subjected to 240 °C crystallization for longer than 1 min, P2 and P4 start to appear and become increasingly evident upon DSC scanning. The intensity (P2 and P4) initially increases continuously with longer crystallization times up to about 5 min, beyond which the intensity gradually stabilizes at a fixed value.

On the other hand, the origin of P3 and the shoulder P4 is yet to be understood. As P2 and P4 appear almost simultaneously, it is proposed that P2 and P4 are associated with the α -crystal. For the same reason, it is proposed that P1 and P3 are the melting endotherms for the β -crystal. Further evidence will be searched for proof, and more details will be discussed in later sections. Thus, during the melt-crystallization process, the growth of the α -crystal lags behind the β -type crystal as the molten sPS is brought to an isothermal crystallization temperature. During melt-crystallization, the β -crystal is a thermodynamically preferred way of packing. On the other hand, the α -type crystal may be a convenient alternative kinetic mechanism of molecular packing for stiffened sPS chains with reduced molecular mobility in partially solidified sPS.

Characterization of Crystal Forms. Chain intermixing in polymer–polymer miscibility leads to a thermodynamic state of sPS favoring predominant formation of β -crystal and depressed fraction of α -crystal.^{8,28,29} Guerra et al. also have found that the polymorphism behavior of sPS in its mixtures with poly(1,4-dimethylphenylene oxide) (PPO) is significantly different from that of neat sPS.²⁸ Further evidence was searched for. As the T_g of miscible sPS/PPO can be significantly different from neat sPS, this study chose to use the miscible blend of aPS/sPS, whose miscibility has been proven,²⁶ as a model owing to proximity of these two polymer T_g 's. Figure 2 shows the X-ray diffractograms for (a) neat sPS sample, in comparison with (b) aPS/sPS (1:1) blend. Prior to X-ray characterization, both samples were melt-crystallized at exactly the same temperature of 240 °C for the same time of 120 min.

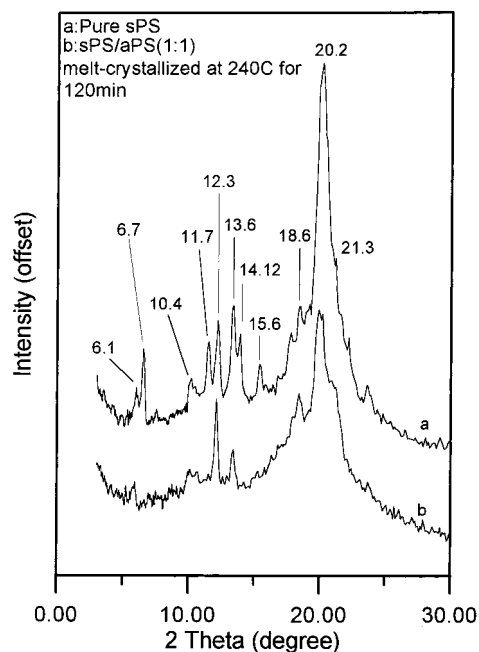


Figure 2. X-ray diffractograms for (a) neat sPS sample and (b) aPS/sPS (1:1), with both samples having been melt-crystallized at 240 °C for 120 min.

The figure shows that diffraction peaks for the sPS (diffractogram a) are at $2\theta = 6.1, (6.7), 10.4, (11.7), 12.3, (13.6), 14.2, (15.6), 17.8, 18.6, 20.2,$ and 21.3° . The diffraction peaks in parentheses indicate those typical of the α -crystal.^{3,4} Characteristic peaks of the β -crystal form (De Rosa et al.,^{4–6} $2\theta = 6.1, 10.4, 12.3, 13.6, 18.6, 20.2,$ and 21.4°) are seen in this melt-crystallized sPS. Note that the peak at 20.2° is characteristic of both α - and β -forms, and therefore it is seen in sPS regardless of thermal treatment. Obviously, the 240 °C melt-crystallized neat sPS contains both α - and β -crystals. On the other hand, X-ray characterization on aPS/sPS (1:1) yielded a diffractogram (Figure 2b) with much fewer diffraction peaks, suggesting a reduced number of crystal forms in aPS/sPS as a result of miscibility with aPS. Figure 2b for the aPS/sPS blend sample shows that diffraction peaks are seen at $2\theta = 6.1, 10.4, 12.3, 13.6, 18.6, 20.2,$ and 21.4° , which are mostly β -crystal with characteristic peaks for the α -crystal all disappearing.

Similarly, X-ray characterization was performed on the neat sPS and aPS/sPS blend (1:1) sample thermally treated at a different temperature. Again, prior to X-ray characterization at ambient temperature, both samples were fully melt-crystallized at exactly same temperature of 250 °C for same time of 120 min. Figure 3a,b shows the X-ray diffractograms for (a) neat sPS sample, in comparison with (b) aPS/sPS (1:1). A similar trend is seen in that the 250 °C melt-crystallized neat sPS exhibits diffraction peaks that show characteristics of both α - and β -crystals, while the crystalline phase in the aPS/sPS (1:1) blend is characterized by the β -crystal only. These X-ray results yielded evidence that the β -crystal (orthorhombic unit cell) may dominate the crystalline domain of melt-crystallized miscible aPS/sPS blend, but both α - and β -crystals can coexist in melt-crystallized sPS.

In addition, a direct comparison of neat sPS melt-crystallized at 240 and 250 °C (Figures 2a and 3a) show that both α - and β -crystal diffraction peaks are seen in the neat sPS, but melt-crystallization at higher tem-

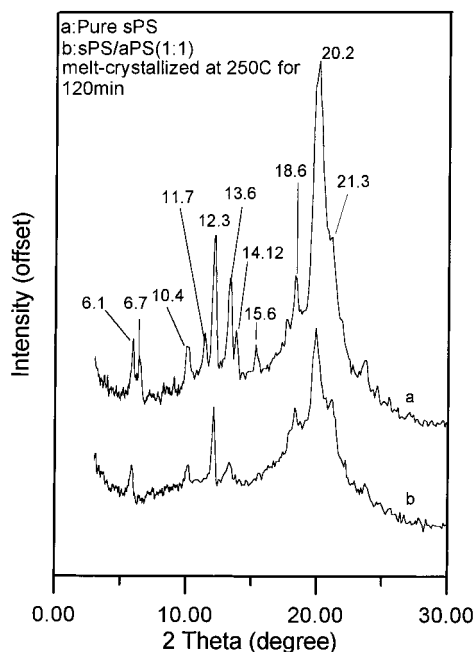


Figure 3. X-ray diffractograms for (a) neat sPS sample and (b) aPS/sPS (1:1), with both samples having been melt-crystallized at 250 °C for 120 min.

temperatures yielded β -crystal diffraction peaks of greater intensity but α -crystal peaks of reduced intensity. This fact suggests that melt-crystallization at higher temperatures favors β -crystal packing. These changes in the X-ray diffraction results agree with the trend of variation of the thermal behavior as revealed by the DSC characterization. It has been shown⁸ that melt crystallization at temperatures higher than 240 °C can lead to a reduced number of melting peaks as well as changes of peak temperatures. The reduced melting peaks may suggest that one of the crystal forms is likely depressed at higher crystallization temperatures.

DSC characterization was performed on the aPS/sPS blend (1:1) to reveal its melting behavior in comparison with that for the neat sPS having been subjected to exactly the same thermal histories. Figure 4a–f shows the DSC traces (scanned at 5 °C/min) for the aPS/sPS blend melt-crystallized isothermally at 240 °C for various times ranging from 0.5 to 30 min (six samples total). Surprisingly and interestingly, only two melting peaks, not four, are observed (at 259 and 269 °C) in all aPS/sPS blends. Apparently, a careful analysis of peak positions showed that these two melting peaks correspond to P1 and P3, respectively, with P2 and P4 being absent from the DSC traces. Note that initially a trace amount of P2 can be observed in aPS/sPS samples crystallized for a short time (<0.7 min), but for samples crystallized for times longer than 1 min, P2 is overwhelmed by the rapidly increased intensity of P3. Changing the DSC heating scan to lower rates and thus higher resolutions did not reveal more melting peaks, except that at much higher rates these two peaks merged into one endotherm owing to reduced resolution. The DSC result clearly suggests that, in the miscible aPS/sPS subjected to melt crystallization, only the β -form lamella is favored to grow more readily, with α -crystal packing mostly suppressed. These two melting peaks could be initially observed in the samples subjected to crystallization time (at 240 °C) as short as 0.5–0.7 min. In the miscible aPS/sPS blend, the α -crystal

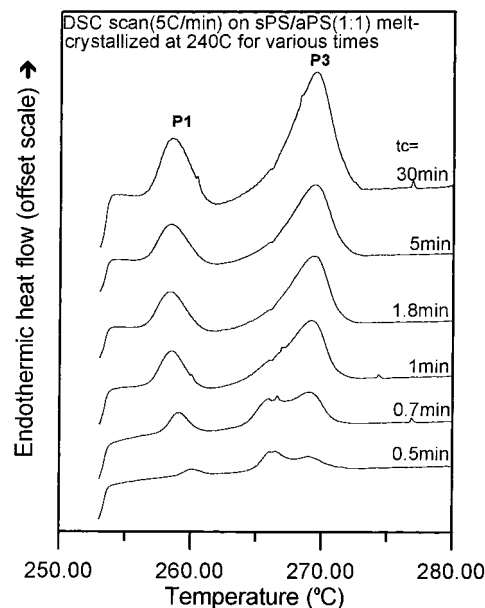


Figure 4. DSC traces (5 °C/min) for the aPS/sPS blend melt-crystallized isothermally at 240 °C for various time duration from 0.5 to 30 min (six samples total).

does not form after the earlier formation of β -crystal in a sequential order, in contrast to the fact that both crystal forms can be present (in various fractions) in the melt-crystallized neat sPS. From the trends and evidence of the DSC and X-ray data, it can be tentatively proposed that P2 and P4 are both attributed to melting of the α -crystal, while melting of the β -crystal yields P1 and P3.

The relationship between P1 and P3, however, requires further interpretation. We thus performed DSC scanning (different rates) on the blend samples containing only β -type. Before DSC experiments of different heating rates, the blend samples were previously melt-crystallized at 240 and 250 °C for 2 h (in DSC cells). Figure 5A,B shows the DSC thermograms for the aPS/sPS (1:1) blend samples scanned at different heating rates (2.5–40 °C/min). Diagram A shows the summary of the DSC traces of the 240 °C crystallized aPS/sPS blend sample, and diagram B shows a similar summary of the DSC traces of the 250 °C crystallized aPS/sPS blend sample. Apparently, P1 becomes more intense and moves to a higher temperature with increasing heating rates; P3, however, diminishes to a less visible endotherm (by comparison to the intensity of P1) with increasing rates. In addition, the temperature position of P3 remains approximately the same regardless of the heating rates. From the observation, it is proposed that P1 and P3 are associated with melting of the originally packed thin and thick β -form crystal lamellae, respectively. Furthermore, the originally thin β -form crystal lamellae can be melted and recrystallized to thicker lamellae of the same β -form. Upon heating scans, the lamellae that are melted to show P1 can be recrystallized and reorganized into thicker lamellae. That is, originally thin lamella of the β -crystal melts first to yield P1 upon scanning; subsequently, the melted polymer liquid is reorganized into thicker lamellae (with unaltered β -crystal packing), as long as the heating scan rate is not too fast. Upon scanning to higher temperatures, the thickened β -crystal lamella is eventually melted again to yield P3. Thus, P1 and P3 are both associated with melting of the β -type crystal lamella, but P3 may

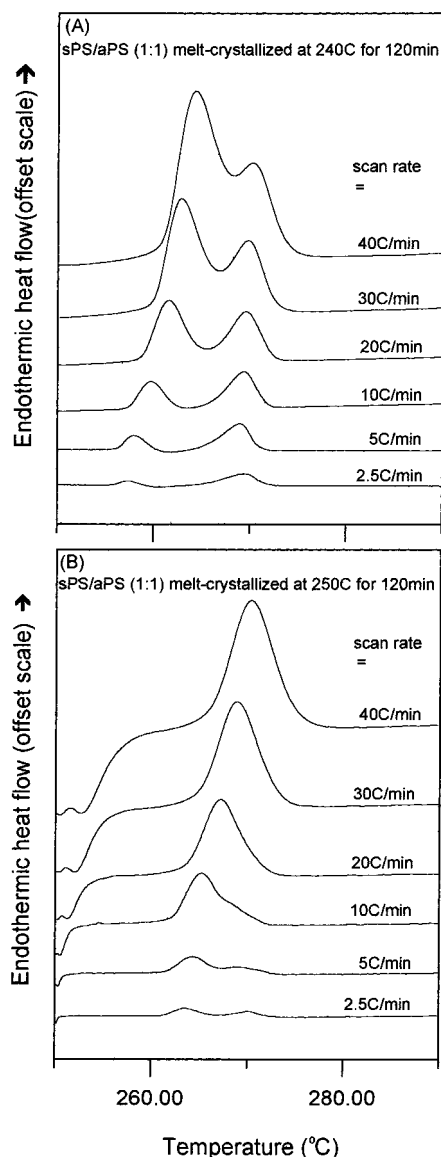


Figure 5. DSC thermograms for miscible aPS/sPS (1:1) blend samples scanned at different heating rates (2.5–40 °C/min, as-labeled): (A) samples previously melt-crystallized at 240 °C and (B) samples previously melt-crystallized at 250 °C for 2 h.

be a superimposed melting endotherm representing both originally thick β -form lamellae and the recrystallized (originally thinner) and scanning-thickened lamellae of the β -crystal.

Furthermore, as evidenced in the X-ray result, low-temperature melt-crystallization does not favor formation of the β -crystal in sPS. As a result, the α -crystal exists in comparatively higher fractions in the low-temperature melt-crystallized sPS. To prove its thermal behavior, DSC was performed on the neat sPS samples melt-crystallized at 230 °C for various times from 0.1 to 30 min. Note that greater experimental difficulty was experienced if one attempted to perform melt-crystallization at temperatures lower than 230 °C. This was so because sPS naturally crystallizes extremely fast; thus, quenching to isothermal crystallization farther down from the melt temperature would involve uncertain extents of dynamic cooling-induced crystallization.

Recrystallization/Remelting of β -Crystal Lamellae. Figure 6a–f shows the DSC traces (all scanned at

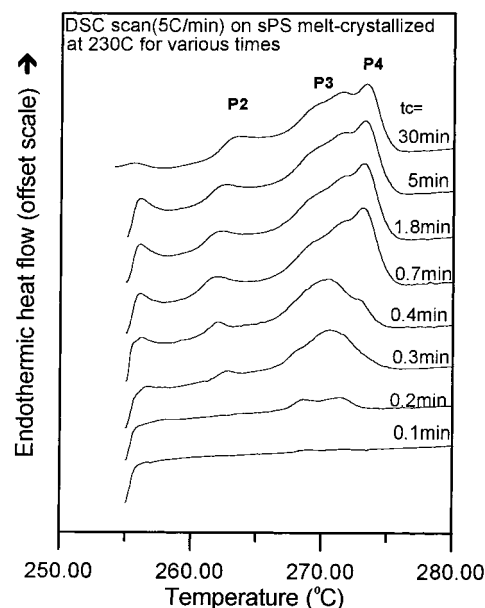


Figure 6. DSC traces (5 °C/min) for the aPS/sPS blend melt-crystallized isothermally at 230 °C for various times from 0.5 to 30 min (six samples total).

5 °C/min) for the sPS blend melt-crystallized isothermally at 230 °C for various times ranging from 0.5 to 30 min (eight samples total). Interestingly, P3 was temporarily dominant for the samples 230 °C melt-crystallized for times less than 1 min, but then for longer times P4 eventually overtook it. But for samples eventually crystallized for longer times at 230 °C, only two “prominent” peaks (P2 at 263 °C and P4 at 272–273 °C) are seen, with P3 being negligible. Especially, P4 (at 273 °C) becomes more evident in the 230 °C-crystallized sPS samples. P1 is absent from all DSC traces, and P3 only appears as a broad endotherm (~270 °C) just below the more evident P4. According to the proposed assignments, the absence of P1 and reduced P3 intensity together provides additional evidence that crystal packing of the β -form is likely hindered to a greater extent in the melt-crystallized sPS at lower crystallization temperatures (230 °C or lower). On the other hand, when the crystallization temperature is low, the mechanism of the α -form packing becomes a kinetically favored alternative, owing to hindered packing of the β -crystal (P1, P3), leading to a more pronounced P4.

Figure 7 shows a direct comparison of the melting behavior (10 °C/min) of sPS having been isothermally melt-crystallized at (diagram A) 260 °C and (diagram B) 230 °C, both for the same extended time of 240 min (4 h). The 260 °C crystallized sPS exhibits a single sharp melting peak at 272 °C with a minor broad shoulder at 276 °C. The large sharp melting peak (272 °C) represents a merged endotherm of P1 and P3 (β -crystal), while the minor shoulder is melting of trace α -crystal. The 230 °C crystallized sPS exhibited distinctly different melting features from those of 260 °C crystallized in that all four melting peaks (P1, P2, P3, and P4) are clearly present. As discussed earlier, the melting behavior indicates that 260 °C crystallization leads to a much smaller fraction of α -crystal than 230 °C crystallization.

On the other hand, melt-crystallization at high temperatures (e.g., 260 °C or higher) preferentially favors β -form packing in sPS to an extent that α -form packing does not proceed. Figure 8 shows the X-ray diffractogram for neat sPS melt-crystallized at 260 °C for 120

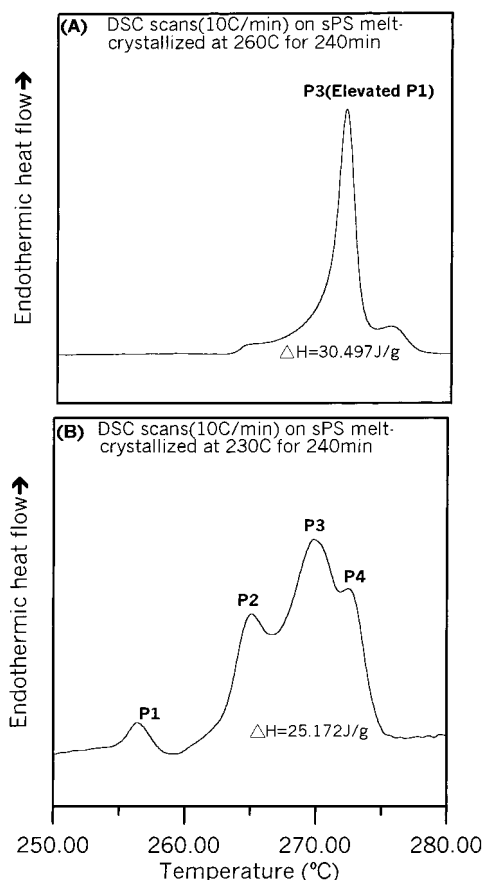


Figure 7. Comparison of the melting behavior (DSC scanning at 10 °C/min) of sPS having been isothermally crystallized at (A) 260 and (B) 230 °C for 240 min.

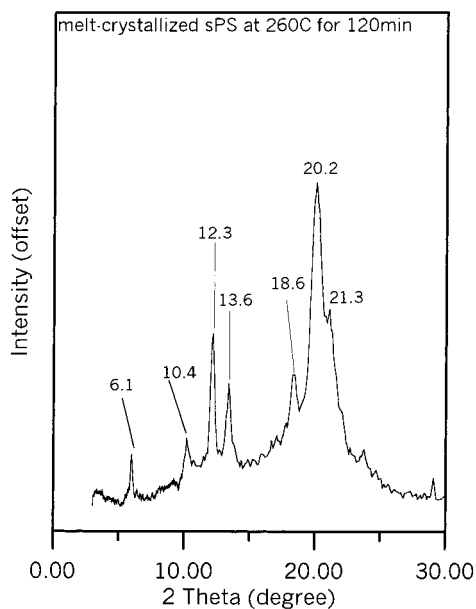


Figure 8. X-ray diffractogram for neat sPS melt-crystallized at 260 °C for 120 min, showing only characteristic β-crystal peaks.

min. Interestingly, the number of diffraction peaks in this neat sPS sample is significantly reduced. Characteristic peaks of $2\theta = 6.1, 10.4, 12.3, 13.6, 18.6, 20.2,$ and 21.4° are evidently of the β-crystal in this 260 °C melt-crystallized sPS, while all α-crystal diffraction peaks are absent from this sample. Obviously, the 260 °C melt-crystallized neat sPS contains only the β-crys-

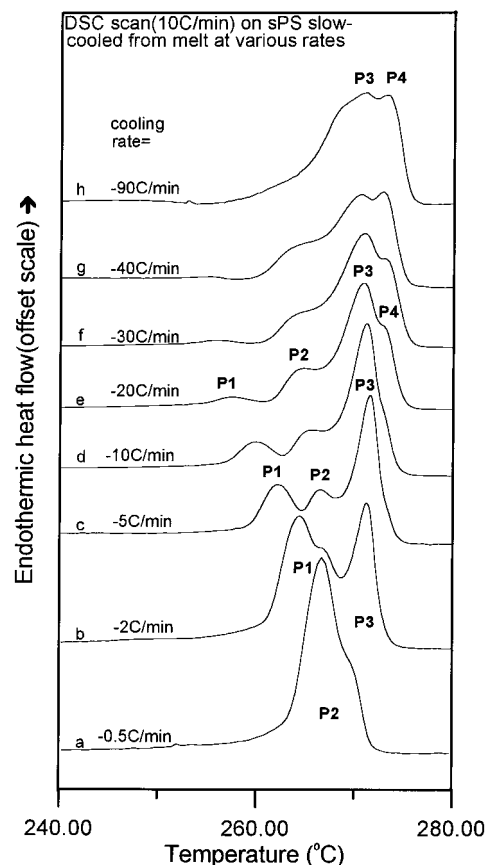


Figure 9. DSC traces (scanned at 10 °C/min) for the neat sPS having been dynamically cooled at various rates from very slow to fast cooling (from bottom to top, as labeled).

tal, which is in excellent agreement with the interpretation based on the DSC results.

Individual lamellae of β-form can be thickened upon heating or annealing, but the α-crystal packed lamellae cannot be thickened. Either the α-form lamellae are melted and gone during dynamic scanning, or they are gradually transformed (repacked) to β-form lamellae upon extended annealing at sufficiently high temperatures. The thickening phenomenon of the β-form lamella upon isothermal annealing or dynamic scanning is especially apparent for the originally thin lamella of P1. An earlier related study⁸ also shows that, for melt-crystallized sPS samples subjected to postannealing at a high temperature (between 240 and 260 °C) for extended times, P2 (α-type) intensity diminishes, but the intensity of P1 (thin lamella of β-type) increases and eventually is elevated to merge with P3.

Effect of Dynamic Cooling Rates. As discussed, the melt crystallization temperature can exert significant effects on relative fractions of crystal forms as well as the lamellar thickness. When cooled at slow rates, the crystallizing chains are packed into crystals at high temperatures for longer times. Vice versa, when subjected to faster cooling rates, the polymer chains being packed into crystals would spend more time at low temperatures. A series of sPS samples were prepared by slow cooling (from the molten state) at various rates ranging from very slow (−0.5 °C/min) to very fast (−90 °C/min) cooling. Then, DSC scanning was performed on these samples, all at a same scanning rate of 10 °C/min. Figure 9 shows the DSC traces (scanned at 10 °C/min) for the neat sPS samples having been dynamically cooled at various rates from very slow to fast cooling

(from bottom to top, as labeled). The slowest cooling rate ($-0.5\text{ }^{\circ}\text{C/min}$, thermogram a) imposed on sPS led to a sharp melting peak at $267\text{ }^{\circ}\text{C}$ and a partially merged shoulder peak at $270\text{ }^{\circ}\text{C}$. These two melting peaks in the sPS (dynamically cooled at $-0.5\text{ }^{\circ}\text{C/min}$) correspond to P1 and P3, respectively, in isothermally crystallized sPS. Note that P1 in this slow-cooled sPS is significantly larger and located at a considerably higher temperature than those commonly observed in a melt-crystallized sPS (e.g., $240\text{ }^{\circ}\text{C}$, crystallized). This is due to an annealing effect that led to extended thickening of the lamella of P1. During an extremely slow cooling scheme ($-0.5\text{ }^{\circ}\text{C/min}$, thermogram a), the crystallizing sPS molecules were subjected to higher temperatures during most of its crystallization process. As most β -form lamellae have been sufficiently thickened during the very slow cooling, only relatively little of these thickened lamellae would be available for melting and recrystallization to even thicker lamellae (which would melt to give peak 3) upon DSC scanning at $10\text{ }^{\circ}\text{C/min}$. Thus, P3 appeared as a small shoulder endotherm in this sample. The melting behavior of this slow-cooled sPS sample suggests that the main crystalline domain is of β -form if sPS is cooled very slowly. If imposed to a 10 times higher cooling rate ($-5\text{ }^{\circ}\text{C/min}$, thermogram c), the cooled sPS yielded three observable peaks: P1, P2, and P3. The trend indicates that the α -form becomes increasingly more visible if faster rates were used in cooling the sPS. In addition, the melting endotherm of P1 for the $-5\text{ }^{\circ}\text{C/min}$ slow-cooled sPS is of a lower intensity, and P1 is located at a lower temperature than those observed in the $-0.5\text{ }^{\circ}\text{C/min}$ cooled sPS. This clearly suggests that faster cooling on sPS exerted a relatively lesser effect of annealing. If an intermediate cooling rate ($-20\text{ }^{\circ}\text{C/min}$, thermogram e) was imposed on sPS, the dynamically cooled sPS exhibited all four melting peaks, although the peaks possess less sharpness in comparison to those in the melt-crystallized counterpart. If subjected to fast cooling rates ($-90\text{ }^{\circ}\text{C/min}$, thermogram h), the fast-cooled sPS exhibited melting endotherms that are composed of partially merged broad P3 and relatively sharp P4. Thus, except for very slow cooling, most dynamically cooled sPS would contain a combination of α - and β -crystals, but crystallization at higher cooling rates is more inducing for α -crystal packing.

The fast-cooled sPS thus was expected to contain a greater fraction of α -crystal than the slow-cooled sPS. Figure 10 shows the X-ray diffractograms for the neat sPS having been dynamically cooled at (a) -0.5 , (b) -2 , (c) -10 , (d) -40 , and (e) $-90\text{ }^{\circ}\text{C/min}$. In agreement with the DSC result of the previous figure, the X-ray result shows that the diffraction peaks in the very slowly cooled sPS sample ($-0.5\text{ }^{\circ}\text{C/min}$, diffractogram a) are all of β -form only ($2\theta = 6.1, 10.4, 12.3, 13.6, 18.6, 20.2$, and 21.4°), with all α -crystal diffraction peaks being absent. This extremely slow-cooled sPS possesses all characteristic diffraction peaks that are similar to the $260\text{ }^{\circ}\text{C}$ melt-crystallized sPS (all β -form, see Figure 8), indicating that the β -crystal is the only favored packing in extremely slow-cooled sPS as well as in high-temperature crystallized sPS. However, when cooled at increasingly faster rates, the relative fractions of crystal types in dynamically cooled sPS samples were different. Thermograms b–e clearly show that both the α - and β -form are present in most dynamically cooled sPS samples (cool rate ranging from -2 to $90\text{ }^{\circ}\text{C/min}$)

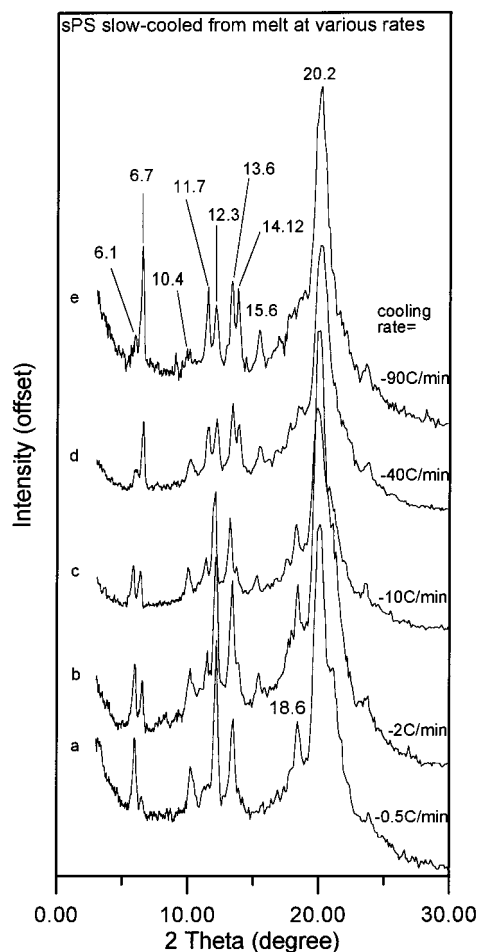


Figure 10. X-ray diffractograms for neat sPS having been dynamically cooled at (a) -0.5 , (b) -2 , (c) -10 , (d) -40 , and (e) $-90\text{ }^{\circ}\text{C/min}$.

and that the characteristic α -crystal diffraction peaks ($2\theta = 6.7, 11.7^{\circ}$) become more evident with faster cooling rates. Apparently, the cooling rate (from the molten state) in a dynamic cooling scheme from the molten state has a similar effect on the temperature in an isothermal crystallization scheme. As evidently demonstrated in this study, the dynamic cooling rate can lead to a preferential type of crystal packing.

Similar dynamic cooling schemes of various rates were imposed on the aPS/sPS blends, and their melting behavior and crystal forms were examined in order to compare with the results for the neat sPS subjected to the same thermal histories. Figure 11 shows the DSC traces (scanned at $10\text{ }^{\circ}\text{C/min}$) for the aPS/sPS samples having been dynamically cooled at various rates from very slow to fast cooling (from bottom to top, as labeled). The extremely slow-cooling ($-0.5\text{ }^{\circ}\text{C/min}$) aPS/sPS blend yielded a single sharp melting peak at $266\text{ }^{\circ}\text{C}$. A shoulder peak may have been partially merged in this peak. The melting behavior of this aPS/sPS blend (1:1) is similar to the neat sPS dynamically cooled at the same rate ($-0.5\text{ }^{\circ}\text{C/min}$). Surprisingly, however, the aPS/sPS blend samples subjected to higher cooling rates (-2 to $-90\text{ }^{\circ}\text{C/min}$) did not show any traces of melting behavior that are characteristic of the α -form crystal. This is in distinct contrast with the result for the neat sPS. As earlier shown in previous figures (Figures 9 and 10), it is clear that both α - and β -crystals are present in most transient-cooled neat sPS unless an extremely slow rate was used ($-0.5\text{ }^{\circ}\text{C/min}$ or lower).

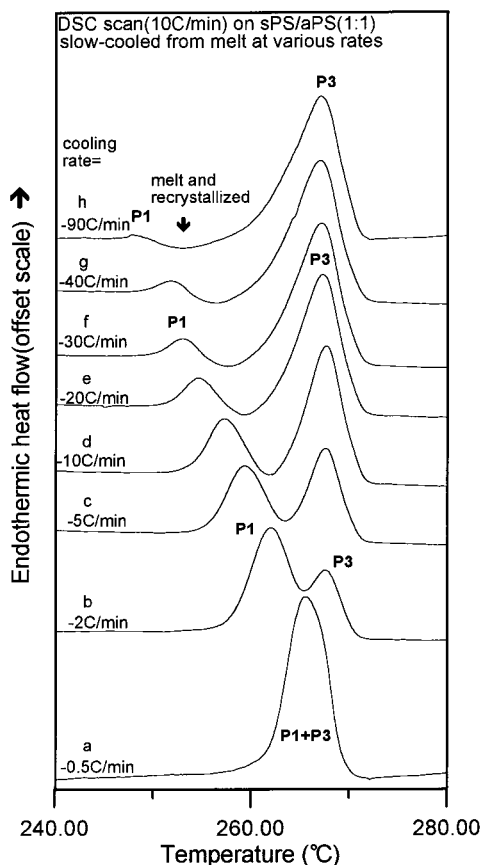


Figure 11. DSC traces (scanned at 10 °C/min) for the aPS/sPS samples having been dynamically cooled at various rates from very slow to fast cooling (from bottom to top, as labeled).

Again to support the previous analysis, X-ray characterization was performed on the transient-cooled aPS/sPS blends that had been subjected to cooling from the molten state at various rates. Figure 12 shows the X-ray diffractograms for the aPS/sPS blend (1:1) having been dynamically cooled: (a) -0.5 , (b) -2 , (c) -10 , (d) -40 , and (e) -90 °C/min. Regardless of the rates (very slow to fast) used in cooling the aPS/sPS blend from the molten state, all aPS/sPS blend samples exhibit only diffraction peaks characteristic of the β -form crystal ($2\theta = 6.1, 10.4, 12.3, 13.6, 18.6, 20.2$, and 21.4°), and no α -crystal diffraction peaks are observed. This is very different from that observed in the cooled neat sPS samples, where combination of different fractions of α - and β -forms are observed, depending on the cooling rates. Thus, once again the above DSC and WAXD results for the cooled aPS/sPS blend samples show that the α -crystal is not the favored crystal packing for the sPS molecules in a miscible state with other polymer chains. By using the miscible aPS/sPS blend as a model and by eliminating one of the crystal forms in sPS, the origin and assignment of the melting peaks in sPS were made more straightforward.

Conclusion

This study has provided evidence of details for interpretation of the multiple melting and polymorphism crystals in sPS. For the first time, assignment of different crystal types to the numerous melting peaks was accomplished with sufficient proof. Effects of temperature and thermal histories on the mechanism of chain packing were examined for correlating the rela-

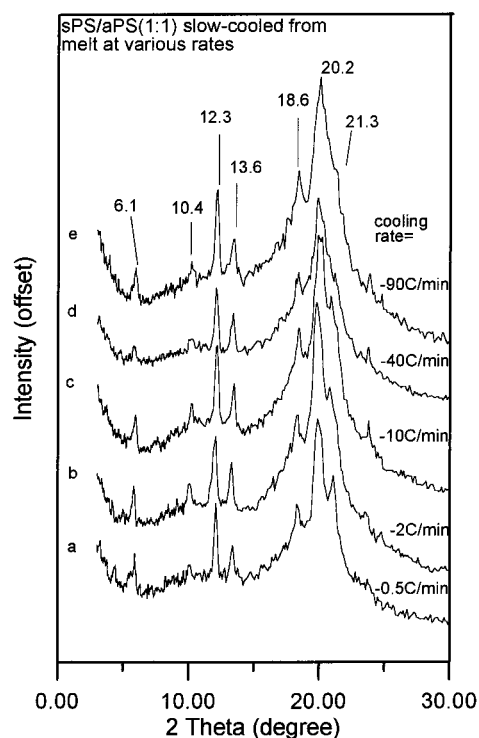


Figure 12. X-ray diffractograms for the aPS/sPS blend (1:1) having been cooled at (a) -0.5 , (b) -2 , (c) -10 , (d) -40 , and (e) -90 °C/min.

tionships between the polymorphism and multiple melting peaks. The α -crystal packing can be favored or becomes an alternative route in sPS crystallization under three conditions: (1) slow cooling from the molten state, (2) melt crystallization at low temperatures (e.g., 230 °C or lower), or (3) cold crystallization from quenched glass. As a matter of fact, cold-crystallized sPS samples contain only the α -type crystal,¹ which differs significantly from melt-crystallized sPS in crystal forms or the shapes of melting endotherms. By comparison, melt-crystallization at most accessible temperatures produce solidified sPS containing both α -type (P2 and P4) and β -type (P1 and P3) crystals of various fractions. Generally speaking, the low to medium melt crystallization temperature always results in growth of the β -crystal and α -type, but higher melt-crystallization temperature tends to favor greater fractions of β -type. As a matter of fact, the β -type crystal became the only dominating species if sPS was melt-crystallized at temperatures equal to or higher than 260 °C. A single sharp melting peak was observed upon scanning on the high-temperature-crystallized sPS containing only the β -crystal. Under conditions approaching "equilibrium", only lamellae of the β -crystal are present and are the favored type of packing, with an extrapolated equilibrium melting temperature at $T_m^* = 286.6$ °C.^{8,30}

The melting behavior and stability of these two crystal types are likely different. Under the same thermal histories, the α -type crystal melts at higher temperatures than the β -type. Kinetically, the growth of the α -crystal lags behind the β -type as the molten sPS is brought to a supercooled state to initiate crystallization. When freshly cooled from a molten state, most sPS molecules possess sufficient mobility, and the β -crystal is the main mechanism of packing, to be followed by α -type crystal packing during later stages of melt-crystallization in a partially solidified sPS system. This

suggests that the α -type crystal becomes a convenient alternative mechanism of molecular packing for partially solidified sPS, in which most chains are stiffened or possess a reduced molecular mobility owing to partial crystallinity. Similarly, in cold-crystallization where the sPS molecules are being organized into crystals from an originally rubbery state, the α -crystal is the dominating mechanism of molecular packing as the rubbery sPS chains are comparatively less flexible (more sluggish) than the molten sPS chains in the liquid state. Furthermore, the lamellae of the β -crystal can be thickened upon annealing or remelted/recrystallized into thicker lamellae during scanning at slow heating rates. By comparison, lamellae of the α -crystal cannot be thickened. When the α -crystal is melted during heating scans, the experimental evidence shows that it does not reorganize into thicker lamellae. It simply melts into liquid without recrystallization upon further heating. Further work is needed and is undergoing in order to obtain a more quantitative in-depth view.

Acknowledgment. This work was supported by basic research grants from National Science Council (NSC 87 CPC E006 017, NSC 88 CPC E006 016) of ROC-on-Taiwan. The authors are grateful to Mr. Masahiko Kuramoto of Idemitsu Petrochemicals Co. Ltd. (Japan), who kindly supplied the research-grade sPS material for this study.

References and Notes

- (1) Woo, E. M.; Sun, Y. S.; Lee, M. L. *Polym. Commun.* **1999**, *40*, 4425.
- (2) Sun, Z.; Morgan, R. J.; Lewis, D. N. *Polymer* **1992**, *33*, 660.
- (3) Chatani, Y.; Shimane, Y.; Ijitsu, T.; Yukinari, T. *Polymer* **1993**, *34*, 1625.
- (4) Guerra, G.; Vitagliano, V. M.; De Rosa, C.; Petraccone, V.; Corradini, P. *Macromolecules* **1990**, *23*, 1539.
- (5) De Rosa, C.; Rapacciuolo, M.; Guerra, G.; Petraccone, V.; Corradini, P. *Polymer* **1992**, *33*, 1423.
- (6) De Rosa, C. *Macromolecules* **1996**, *2*, 8460.
- (7) Vittoria, V.; Ruvoilo Filho, A.; De Candia, F. *J. Macromol. Sci., Phys.* **1992**, *B31*, 133.
- (8) Woo, E. M.; Wu, F. S. *Macromol. Chem. Phys.* **1998**, *199*, 2041.
- (9) Evans, A. M.; Kellar, E. J. C.; Knowles, J.; Galiotis, C.; Carriere, C. J.; Andrews, E. H. *Polym. Eng. Sci.* **1997**, *37*, 153.
- (10) Wunderlich, B. In *Macromolecular Physics*; Academic Press: New York, 1976; Vol. 3, p 30.
- (11) Roberts, R. C. *Polymer* **1969**, *10*, 113.
- (12) Blundell, D. J. *Polymer* **1987**, *28*, 2248.
- (13) Lee, Y.; Porter, R. S. *Macromolecules* **1987**, *20*, 1336.
- (14) Huo, P.; Cebe, P. *Colloid Polym. Sci.* **1992**, *270*, 840.
- (15) Bassett, D. C.; Olley, R. H.; Al-Raheil, I. A. M. *Polymer* **1988**, *29*, 1745.
- (16) Cheng, S. Z. D.; Wu, Z. Q.; Wunderlich, B. *Macromolecules* **1987**, *20*, 2802.
- (17) Marand, H.; Prasad, A. *Macromolecules* **1992**, *25*, 1731.
- (18) Lovinger, A. J.; Hudson, S. D.; Davies, D. D. *Macromolecules* **1992**, *25*, 1752.
- (19) Chen, C.-Y.; Woo, E. M. *Polym. J.* **1995**, *27*, 361.
- (20) Ko, T. Y.; Woo, E. M. *Polymer* **1996**, *37*, 1167.
- (21) Ishihara, N.; Seimiya, T.; Kuramoto, M.; Uoi, M. *Macromolecules* **1986**, *19*, 2464.
- (22) Tosaka, M.; Tsuji, M.; Cartier, L.; Lotz, B.; Kohiya, S.; Ogawa, T.; Isoda, S.; Kobayashi, T. *Polymer* **1998**, *39*, 5273.
- (23) Greis, O.; Xu, Y.; Asano, T.; Petermann, J. *Polymer* **1989**, *30*, 590.
- (24) Pradere, P.; Thomas, E. *Macromolecules* **1990**, *23*, 4954.
- (25) De Rosa, C.; Guerra, V. M.; Petraccone, V.; Corradini, P. *Polym. J.* **1991**, *23*, 1435.
- (26) Woo, E. M.; Lee, M. L.; Sun, Y. S. *Polymer*, in press.
- (27) Hong, B. K.; Jo, W. H.; Lee, S. C.; Kim, J. *Polymer* **1998**, *39*, 1793.
- (28) Guerra, G.; De Rosa, C.; Vitagliano, V. M.; Petraccone, V.; Corradini, P. *J. Polym. Sci., Polym. Phys.* **1991**, *29*, 265.
- (29) Guerra, G.; Vitagliano, V. M.; De Rosa, C.; Petraccone, V.; Corradini, P.; Karasz, F. E. *Polym. Commun.* **1991**, *32*, 30.
- (30) Cimmino, S.; Pace, E. D.; Martuscelli, E.; Silvestre, C. *Polymer* **1991**, *32*, 1080.

MA990507Y